Electronic Supplementary Material (ESI) for Chemical Communications.

Support Information

A multi-functional oil/water separator from a selectively pre-wetted superamphiphobic paper

Dengteng Ge,[a] Lili Yang,[a,b] Chenbo Wang,[a] Elaine Lee,[a] Yongquan Zhang[b] and
Shu Yang[a, *]

[a] Department of Materials Science and Engineering, University of Pennsylvania, Philadelphia, PA 19104, USA

[b] School of Transportation Science and Engineering, Harbin Institute of Technology, Harbin 150090, P.R. China

Corresponding author:

shuyang@seas.upenn.edu (Prof. Shu Yang); Tel.: 215-898-9645; Fax: 215-573-2128

Materials

Ethanol, 1,2- dichloroethane (DCE), hexadecane, chloroform, methylene blue (blue dye), oil red-O (red dye), sodium dodecyl sulfate (SDS), and Span 80 were purchased from Sigma-Aldrich. Silica nanoparticles (IPA-ST-UP) were obtained from Nissan Chemical America Corporation, and (heptadecafluoro - 1, 1, 2, 2 - tetrahydrodecyl) triethoxysilane (HDFTES) was purchased from Gelest Inc. KLEENEX® C-Fold towels were purchased from Kimberty-Clark Professional.

Preparation of superamphiphobic paper

Fluorinated nanoparticle solution was prepare according to the procedure reported before.[1] The solution was ultrasonicated (Branson Ultrasonic cleaner, 2210) for 15 min before spray coating on the paper towel using airbrush (G44, Master airbrush) at 20 psi and 10 cm away from the towel. Typically ~0.05 mL spray solution was needed to cover 1 cm^2 paper towel. Then the paper was dried in air at room temperature.

Preparation of oil/water mixtures

Hexadecane (ρ=0.77 g/cm^3) and 1,2-dichloroethane (DCE, ρ=1.25 g/cm^3) were used as light oil and heavy oil, respectively. Water-in- oil (W/O) emulsions (V_{water}:V_{oil} =1:9, 3:7 and 5:5) were prepared by stirring water and oil with 0.3 mg/mL Span 80 at 700 rpm for 20 min. Oil-in-water (O/W) emulsions (V_{water}:V_{oil} =5:5, 7:3 and 9:1) were prepared by stirring water and oil with 0.3 mg/mL SDS at 700 rpm for 20 min.

Oil/water separation

The separation apparatus was set up according to the conventional filtration system.[2, 3] Since the sprayed NP film repelled both water and oil used here (hexadecane and DCE),[1] we first pre-wetted the SA-paper with ethanol, which has lower surface energy than hexadecane and DCE, by gradually dropping 0.5-1 mL ethanol onto the SA-paper. Then 5 mL water was immediately dropped onto the SA-paper to create a water pre-wetted SA-paper for water removal. For oil removal, 5 mL oil (hexadecane or DCE) was dropped onto the ethanol pre-wetted SA-paper. After the water or oil completely permeated though the SA-paper, 50-100 mL free oil / water mixture, O/W or W/O emulsions were poured into the separation apparatus to obtain permeates more than 10 g.

Characterization

Morphology of the coatings was characterized by field emission scanning electron microscopy (FESEM, JEOL 7500F SEM) operated at 15.0 kV. The static water and oil contact angles (SCAs) were measured using the Ramé-Hart standard automated goniometer (Model290) with 5-μL liquid droplets. The rolling angles (RAs) were measured from a home-made tilting stage using 10-μL liquid droplets. Purity of permeate after separating water and hexadecane in free form or in emulsions was measured from weight loss after evaporating water at 65°C for 12 h. The transmission of the permeate was collected from UV-vis-NIR spectrophotometer (Cary 5000, Varian). The size of the emulsion droplets was measured using the optical microscopy (BX 61, Olympus) for droplet size >1 μm and dynamic light scattering (Zetasizer Nano S, Malvern Instruments) for droplet size < 1 μm.

The images of water droplet transportation on water pre-wetted SA-paper under the hexadecane phase was taken by high-speed camera (Phantom v9.0, Vision Research) at 1000 frames per second (f/s).

Table S1. Physical properties of various liquid used in the experiments

Liquid	Density g/cm^3	Surface tension mN/m @20^{o}C	Boiling point °C	Vapor pressure mmHg @20°C
Ethanol	0.79	22.1	78.37	44
Water	1.0	72.8	100	17.5
Hexadecane	0.77	27.5	287	0.0014
1,2-dichloroethane	1.25	38.7	83.5	64
Chloroform	1.48	27.2	61.3	160

Wettability of pre-wetted SA-Paper

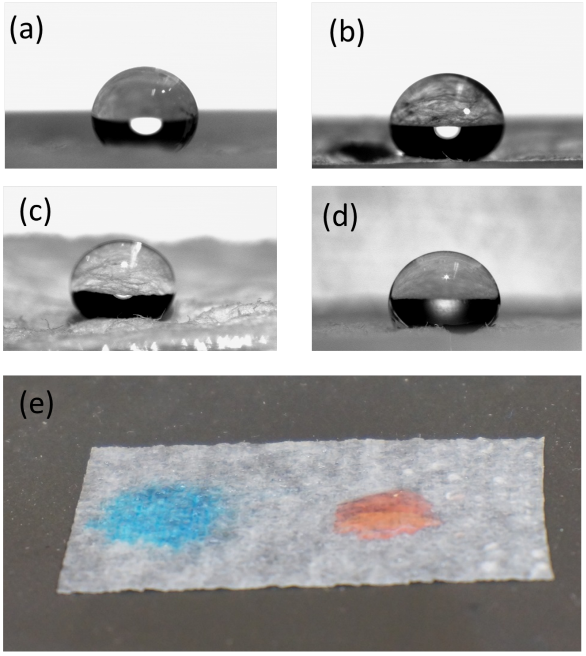

Figure S1. (a) Water and (b) hexadecane droplets on pristine SA-paper with static contact angles of 157.5° and 155.4°, respectively. (c) A hexadecane droplet on water pre-wetted SA-paper with a static contact angle of 145.8° and (d) a water droplet on hexadecane pre-wetted SA-paper with a static contact angle of 143.1°. (e) Optical image of water (blue) and hexadecane (red) spreading on a water pre-wetted pristine paper.

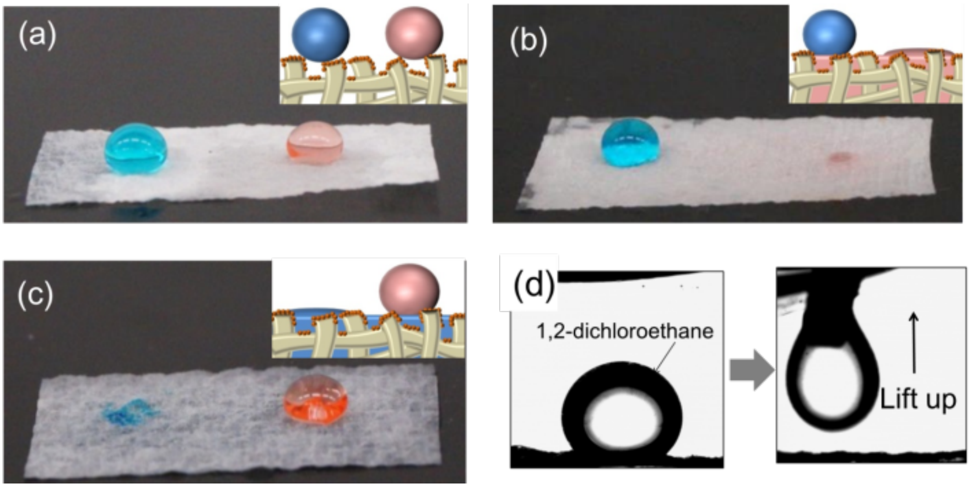

Figure S2. Water (dyed with methylene blue) and hexadecane (dye with red-O) on the (a) SA paper, (b) hexadecane pre-wetted SA-paper and (c) water pre-wetted SA-paper. (d) Optical images of a DCE droplet on the water pre-wetted SA-paper under water, followed by lifting up.

Figures S2b and S2c showed that a water droplet (blue) and a hexadecane droplet (red) sitting on hexadecane and water pre-wetted SA-paper, respectively. Water pre-wetted SA-paper was highly oleophobic (hexadecane SCA = 145.8°, Figure S1c) and superhydrophilic. In contrast, hexadecane pre-wetted SA-paper was superoleophilic and highly hydrophobic (water SCA, 143.1°, Figure S1d). As shown in Figure S2a-c, before pre-wetting, both water and oil droplets were repelled with high mobility on SA-paper in part due to the micro-roughness of the pristine paper and the nano-roughness generated from the NP assembly. After the pre-wetting steps, when placing the liquid droplet same as pre-wetting liquid on the SA-paper, the droplet would be immediately imbibed into SA-paper due to capillary force. Conversely, SA-paper would repel the liquid if it had a very different surface energy from that of the pre-wetting liquid. As seen in Figure S2d, the DEC droplet could be completely lifted up by a plastic pipet tip even though the apparent liquid contact angle on the pre-wetted SA-paper was less than 150^{o}, which could be explained by the replacement of air pocket with higher surface energy pre-wetting liquid (see insets in Figure S2b-c).

Disjoining pressure at water-oil -water interface

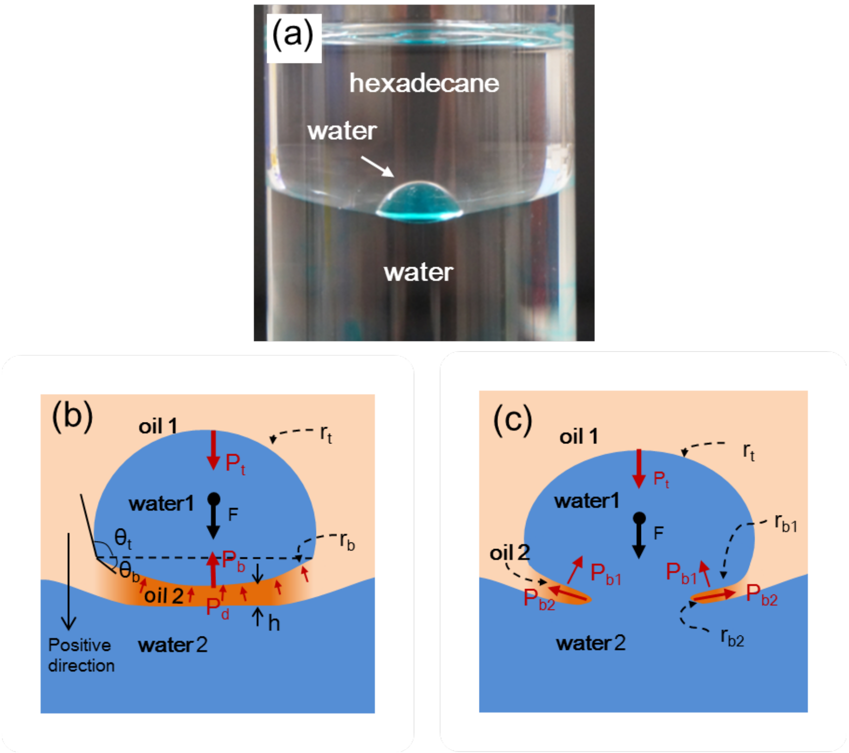

Figure S3. (a) Optical image of water droplet (blue) stabilized at the hexadecane/water interface. (b-c) Illustration of (b) stabilized and (c) ruptured water droplet at the hexadecane/water interface.

The stabilization of water droplets at the water/hexadecane interface could be attributed to the existence of an ultrathin hexadecane film (oil phase 2) between the water phases 1 and 2 (see Figure S3b). Here, the oil phase 2 is also referred as the disjoining layer described by the augmented Young- Laplace equation as[4]

$$P_b = -\frac{2\,\gamma^{w1/O2} cos\theta_b}{r_b} + P_d \qquad (1)$$

where P_b is the capillary pressure (difference in pressure between water phase1 and oil phase 2). It is negative for convex surface. $\gamma^{w1/O2}$ is the interfacial tension between water phase1 and oil phase 2, θ_b is the contact angle between water phase 1 and oil phase 2, r_b is the radius of curvature of water droplet on oil phase 2, and P_d is the disjoining pressure in oil phase 2. $\frac{2\,\gamma^{w1/O2} cos\theta_b}{r_b}$ is the pressure caused by the surface curvature between water phase 1 and oil phase 2. Disjoining pressure results from the interaction between van der Waals force and the electrostatic double-layer when the thickness of oil films is less than 100 nm. At a given temperature and chemical composition of the fluids, the disjoining pressure depends on the thickness and the geometry of the film and describes as [5]

$$P_d = -\frac{A(4-3h_x^2+3hh_{xx})}{24\pi h^3} \tag{2}$$

where A is the Hamaker constant for water phases 1 and 2 interacting through oil phase 2, h, $h_x$and h_{xx} are the oil film thickness, slope and second order derivative of films, respectively. The two interfaces, that is water phase 1- oil phase 2 and oil phase 2 - water phase 2, are nearly parallel, so h_x= h_{xx}= 0 and the disjoining pressure is reduced to

$$P_d = -\frac{A}{6\pi h^3} \tag{3}$$

The difference in pressure of the top curvature of the water droplet P_t is

$$P_t = \frac{2\,\gamma^{w1/O1} cos\theta_t}{r_t} \tag{4}$$

where $\gamma^{w1/O1}$ is the interfacial tension between water phase1 and oil phase 1, θ_t is the contact angle of between water phase 1 and oil phase 1, r_t is the radius of curvature of water droplet at oil phase 1. The force (F) caused by the gravity (G) and buoyancy ($\mathrm{F_{buoy}}$) is given by $F = G - F_{buoy}$. The water droplet (water phase 1) on the thin oil film (oil phase 2) is stable as a result of balancing various forces

$$\mathrm{F} + P_t S_t + P_b S_b = 0 \tag{5}$$

where S_t and S_b are the interfacial area of the water droplet at two oil interfaces. When h is large, disjoining pressure is small, thus P_b+ P_t <0 and P_b+ P_t could not balance the downward force F, leading to the rupture of the oil film. When the oil film (oil phase 2) is thinner than the critical thickness h_c, disjoining pressure is large, leading to increase of P_b and a stable water droplet at the water/oil interface.

Rupture of the disjoining layer

At a given temperature, the magnitude of the disjoining pressure depends on the film thickness, contact angle, and the geometry of the disjoining layer. According to Eq. *2*, the disjoining pressure depends on the slope of films (h_x), while hh_{xx} becomes negligible due to the thin thickness of disjoining layer (h). On a roughness surface, at different locations of disjoining layer, there is variable h_x, thus variable disjoining pressure. Therefore, the disjoining layer is unstable on a hierarchically rough surface. Simulation of disjoining layer profile on microstructures also shows disjoining layer would rupture on tops of the rough surfaces.[6] Once the disjoining layer is ruptured at a certain point of the oil/water interface, water phase 1 and water phase 2 become connected, forming a new water - oil interface (see Figure S3c). The water droplet (water phase 1) quickly migrates into water phase 2 due to the downward pressure (P_t) and increases water phase connection caused by capillary pressure produced by the new curvature at the rupture point (P_{b2}).

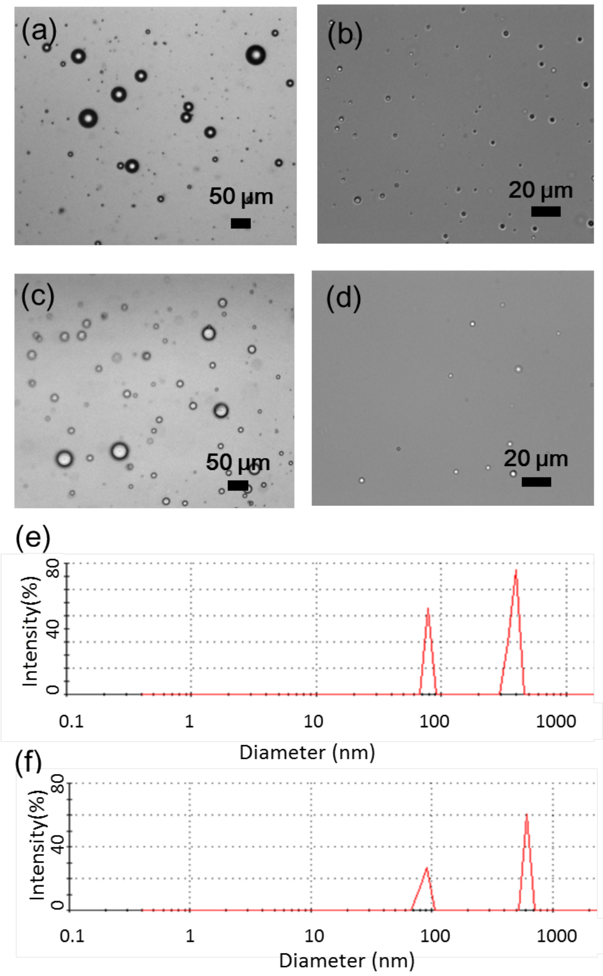

Figure S4. Optical microscopy images of hexadecane-in-water emulsions (V_{water}:$V_{hexadecane}$=7:3) (a) before and (b) after separation on water pre-wetted SA-paper. (c, d) Optical microscopy images and (e, f) dynamic light scattering spectra of water-in-DCE emulsions (V_{water}:V_{DCE} =3:7) before (c, e) and after (d, f) separation on DCE pre-wetted SA-paper.

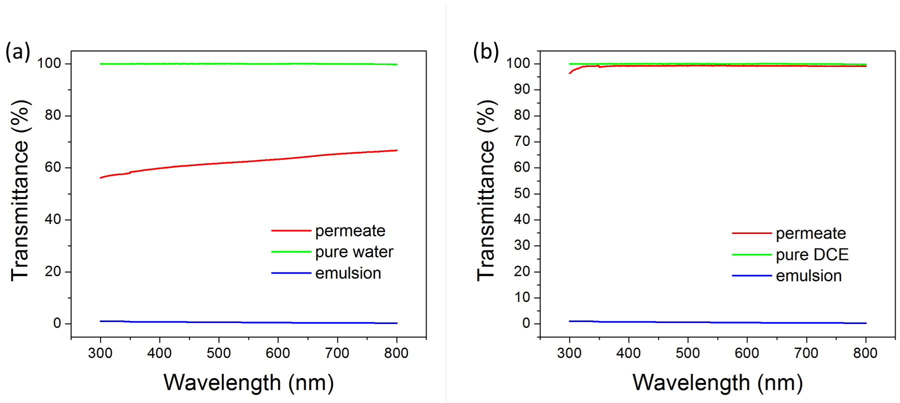

Figure S5. Transmittance of emulsions and permeates separated from (a) water-in-hexadecane emulsions (V_{water} : $V_{hexadecane}$=3:7) and (b) water-in-DCE emulsions (V_{water}:V_{DCE} =3:7).

Table S2**.** Hexadecane/water separation efficiency and fluxes of permeates using water pre-wetted pristine paper and SA-paper as separators.

Type of mixture	Separator	Separation efficiency (%)	Flux ($Lm^{-2}h^{-1}$)
Free mixture	Pristine paper	99.93	46,200
(V_{water}:$V_{hexadecane}$=5:5)	SA-paper	99.99	28,600
Emulsion	Pristine paper	99.86	3,260
(V_{water}:$V_{hexadecane}$=7:3)	SA-paper	99.92	4,480

Calculation of breakthrough pressure and breakthrough height

The breakthrough pressure ($P_{breakthough}$) is the pressure for non-wetting liquid passing though the wetted separator. It can be calculated by [7]

$$P_{breakthough} = \frac{2\gamma^{o/w}|cos\theta|}{\overline{d}} \tag{6}$$

The breakthrough height ($h_{breakthough}$) can be calculated by

$$h_{breakthough} = \frac{P_{breakthough}}{\rho g} \tag{7}$$

where $\gamma^{o/w}$ is the oil/water interfacial tension, θ is the contact angle of non-wetting liquid on the wetted SA-paper, $\overline{d}$ is the average pore size of the SA-paper, ρ is the density of remaining liquid and g is the acceleration of gravity. The pore size of the SA-paper ranges from 10 μm to 60 μm. Here, we used the average pore size of 35 μm. The breakthrough heights were measured as 50.9 cm for hexadecane and 20.1 cm for water (see Figure S6), in close agreement with the theoretical values, 54.8 cm and 23.7 cm, respectively (see summary in Table S3).

Table S3. Theoretical values of the breakthrough pressure ($P_{breakthrough}$) and breakthrough height ($h_{breakthrough}$) of the remaining liquid on pre-wetted SA-paper

Remaining liquid	Pre-wetted liquid	$\bar{d}$ (μm)	θ (°)	γ^{o-w} (mN/m)	ρ (g/cm^3)	$P_{breakthrough}$ (kPa)	$h_{breakthrough}$ (cm)
hexadecane	water	35	162	51.4	0.77	4.16	54.8
water	DCE	35	165	27.9	1	2.30	23.7

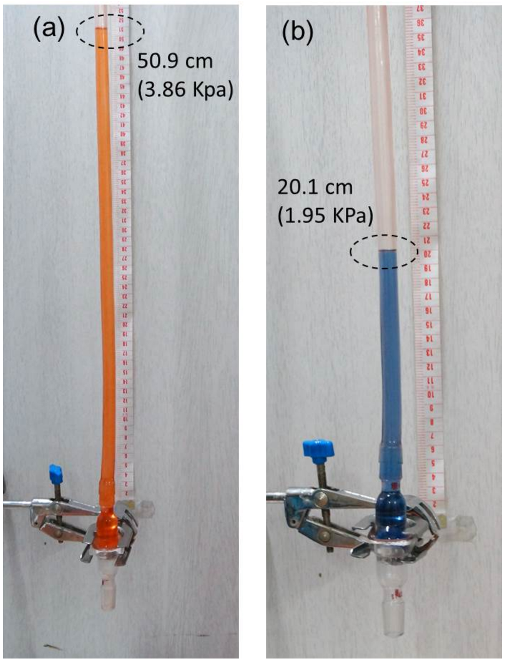

Figure S6. The measured breakthrough height of (a) hexadecane (dyed in red) on water pre-wetted SA-paper and (b) water (dyed in blue) on DCE pre-wetted SA-paper.

We attempted to remove light oil, hexadecane (ρ =0.77 g/cm^3), continuously from its oil–water emulsions. Typically it requires multi-cycles[8, 9] or use of a complex separation machine to prevent the remaining water from covering the separator.[10] Here, we continuously sucked and squeezed the emulsion droplets using a pipette to introduce convection, thus, increasing the contact between hexadecane and the hexadecane pre-wetted SA-paper. It is important that such convection should not breakthrough the pre-wetted hexadecane layer in the SA-paper. Our calculation (see Table S3) and measurement (see Figure S6) showed that the breakthrough pressure and height of the hexadecane wetted SA-paper were ~4 kPa and 50 cm, respectively. Therefore, gentle force such as stirring and sucking/squeezing in our experiments would not overcome this critical pressure. Under forced convection, however, because hexadecane could make continuous contact with the hexadecane pre-wetted SA-paper, the separation of hexadecane from the emulsions was enhanced. As shown in Video S5, hexadecane was immediately separated by the hexadecane pre-wetted SA-paper when the emulsions were poured on top. In contrast, separation stopped after a few seconds when water spread on the hexadecane-wetted SA-paper.

Separation of stable emulsions with low W/O ratio or O/W ratio

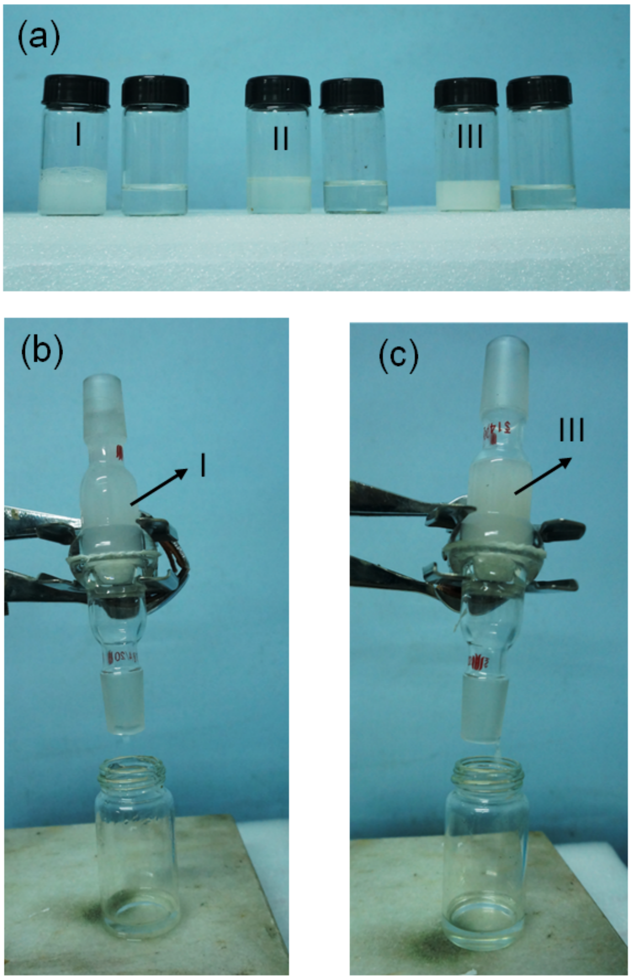

Figure S7. (a) Photos of three different types of emulsions and their permeates. I: hexadecane-in-water with 1 mL hexadecane, 115 mL water, and 0.7g SDS. II: water-in-DCE with 1mL water, 115 mL DCE, and 0.7g Span 80. III: water-in-chloroform with 1 mL water, 115 mL chloroform, and 0.7 g Span80. (b-c) Photos of the separation process of hexadecane-in-water (b) and water-in-chloroform (c).

Water-in- oil (W/O) emulsions with low water concentration and oil-in-water (O/W) emulsions with low oil concentration are highly stable. It has been shown that emulsions prepared by mixing 1 mL water in 115 mL chloroform with 0.7g Span 80, followed by stirring for 3h is stable for more than 90 days.[11] To further explore the separation efficiency of SA-paper, we prepared water-in-chloroform emulsions following the same formula reported in ref. 8. In addition, we prepared water-in-DCE emulsions with 1mL water, 115 mL DCE and 0.7g Span 80, and hexadecane-in-water emulsions with 1mL hexadecane, 115 mL water and 0.7g SDS. After 3h string, the emulsions were collected for separation as shown in Figure 7a. For separation, water pre-wetted SA-paper was used to separate hexadecane-in-water emulsions, and DCE or chloroform pre-wetted SA-paper was used to separate water-in-DCE emulsions or water-in- chloroform emulsions, respectively. As seen in Figure S7b and c, all the permeates were clear liquids. The separation efficiency of hexadecane-in-water emulsions, water-in-DCE emulsions, and water-in-chloroform emulsions were 99%, 99% and 98%, respectively. The flux of those emulsions was determined as 179.4 L/m^{2}h, 174.8 L/m^{2}h and 134.7 L/m^{2}h, respectively.

References

1. D. Ge, L. Yang, Y. Zhang, Y. Rahmawan and S. Yang, *Particle & Particle Systems Characterization*, 2014, n/a-n/a.
2. W. Zhang, Y. Zhu, X. Liu, D. Wang, J. Li, L. Jiang and J. Jin, *Angew Chem Int Ed*, 2014, **53**, 856-860.
3. A. K. Kota, G. Kwon, W. Choi, J. M. Mabry and A. Tuteja, *Nat Commun*, 2012, **3**, 1025.
4. S. Basu and M. M. Sharma, *Journal Of Colloid And Interface Science*, 1996, **181**, 443-455.
5. B. Dai, L. G. Leal and A. Redondo, *Physical Review E*, 2008, **78**, 061602.
6. D. Silin and G. Virnovsky, *Transport Porous Med*, 2010, **82**, 485-505.
7. P. C. Chen and Z. K. Xu, *Sci Rep-Uk*, 2013, **3**:2776.
8. Z. Shi, W. B. Zhang, F. Zhang, X. Liu, D. Wang, J. Jin and L. Jiang, *Adv Mater*, 2013, **25**, 2422-2427.
9. X. Xiao, X. Peng, H. Y. Jin, T. Q. Li, C. C. Zhang, B. Gao, B. Hu, K. F. Huo and J. Zhou, *Adv Mater*, 2013, **25**, 5091-5097.
10. J. Kong and K. Li, *Sep Purif Technol*, 1999, **16**, 83-93.
11. Y. Z. Cao, Y. N. Chen, N. Liu, X. Lin, L. Feng and Y. Wei, *J Mater Chem A*, 2014, **2**, 20439-20443.

Video S1. Transportation of water droplets at the hexadecane/water interface.

Video S2. Transportation of water droplets at the water pre-wetted SA-paper under hexadecane phase captured by high speed camera at 1000 f/s.

Video S3. Gravity-driven water removal from water-in-hexadecane emulsions ($V_{\mathrm{wate:}}V_{\mathrm{hexadecane\ r}}$=3:7) by water pre-wetted SA-paper.

Video S4. Gravity-driven removal of DEC in water-in-DCE emulsions (V_{water} :V_{DCE} =3:7) using DCE pre-wetted SA-paper.

Video S5. Convection-driven removal of hexadecane from water-in-hexadecane emulsions (V_{water} :$V_{\mathrm{hexadecane}}$: =3:7) on hexadecane pre-wetted SA-paper.